Three-dimensional measurement of periodontal support during surgical orthodontic treatment of high-angle skeletal Class III malocclusion: A retrospective study

Hangmiao Lyu,[a] Huimin Ma,[a] Jianxia Hou,[b] Xiaoxia Wang,[c] Yong Wang,[d] Yijiao Zhao,[d] and Xiaotong Li[a]
Beijing, China

Introduction: This study aimed to quantify the periodontal health of incisors during surgical orthodontic treatment in patients with high-angle Class III malocclusion using a cone-beam computed tomography (CBCT) 3-dimensional (3D) reconstruction technique. **Methods:** The sample consisted of 30 patients with high-angle Class III malocclusion (mean age, 20.53 ± 2.86 years). CBCT images were taken before treatment (T0), after presurgical orthodontic treatment, and after treatment (T2). In addition, 3D tooth and alveolar bone models were generated. The root surface area, periodontal ligament (PDL)_Area, and vertical bone level (VBL) around the maxillary and mandibular central incisors were measured. **Results:** The root surface area and PDL_Area of maxillary and mandibular central incisors decreased continuously between T0 and T2 (P <0.01). At T2, mandibular central incisors showed 38.64 ± 13.39% PDL_Area loss, and maxillary central incisors exhibited 21.13 ± 16.48% PDL_Area loss. For mandibular central incisors, the PDL_Area loss caused by VBL loss was significantly greater than that for maxillary central incisors (P <0.01) and significantly greater than the PDL_Area loss caused by root resorption (P <0.01). From T0 to T2, the lingual surface of maxillary central incisors exhibited greater VBL loss than the other 3 surfaces (P <0.01), and the labial and lingual surfaces of mandibular central incisors demonstrated greater VBL loss than proximal surfaces (P <0.01). **Conclusions:** The 3D CBCT reconstruction method provides useful information regarding the periodontal defects of incisors in patients with high-angle skeletal Class III malocclusion. The PDL_Area of maxillary and mandibular central incisors decreased continuously during the treatment. Vertical alveolar bone levels at proximal surfaces appeared to be relatively stable. (Am J Orthod Dentofacial Orthop 2022;162:839-49)

Patients with Class III malocclusion have thinner anterior alveolar bone and more vertical bone loss than Class I patients with normal occlusion,[1] and the alveolar bone thickness of patients with high-angle skeletal Class III occlusion were significantly smaller than those with skeletal Class III average or low angle occlusion and Class I of mandibular incisors.[2] For patients with Class III malocclusion undergoing

[a]Department of Orthodontics, Peking University School and Hospital of Stomatology, and National Engineering Laboratory for Digital and Material Technology of Stomatology, Beijing Key Laboratory of Digital Stomatology, Beijing, China.
[b]Department of Periodontology, Peking University School and Hospital of Stomatology, and National Engineering Laboratory for Digital and Material Technology of Stomatology, Beijing Key Laboratory of Digital Stomatology, Beijing, China.
[c]Department of Oral and Maxillofacial Surgery, Peking University School and Hospital of Stomatology, and National Engineering Laboratory for Digital and Material Technology of Stomatology, Beijing Key Laboratory of Digital Stomatology, Beijing, China.
[d]Center of Digital Dentistry, Peking University School and Hospital of Stomatology, and National Engineering Laboratory for Digital and Material Technology of Stomatology, Beijing Key Laboratory of Digital Stomatology, Beijing, China.
All authors have completed and submitted the ICMJE Form for Disclosure of Potential Conflicts of Interest, and none were reported.

This work was supported by new technology and new therapeutics of Peking University School and Hospital of Stomatology of 2019 (PKUSSNCT-19B04) and the National Program for Multidisciplinary Cooperative Treatment on Major Diseases (PKUSSNMP-201902). This study was approved by the Ethics Committee of Peking University School and Hospital of Stomatology in 2019 (PKUSSIRB-201951168).
Address correspondence to: Xiaotong Li, Department of Orthodontics, Peking University School and Hospital of Stomatology, and National Engineering Laboratory for Digital and Material Technology of Stomatology, Beijing Key Laboratory of Digital Stomatology, 22 Zhongguancun S Ave, Haidian District, Beijing 100081, China; e-mail, xiaotonglee@hotmail.com.
Submitted, September 2020; revised and accepted, July 2021.
0889-5406/$36.00

https://doi.org/10.1016/j.ajodo.2021.07.022

orthognathic surgery, it is important for orthodontists to monitor their periodontal health condition during treatment. Tooth sockets are formed and supported by the periodontal ligament (PDL) and the alveolar bone. The PDL is an aligned fibrous network anchored firmly to the root cementum of the teeth on one side and the alveolar bone of the jaw on the other side.[3,4] It has been proposed that the PDL and alveolar bone are functional units and undergo robust remodeling in orthodontic tooth movement.[5] The morphologic change of the PDL intuitively reflects the effect of vertical bone level[6] and apical root resorption on periodontal support.[7] Moreover, the PDL_Area is associated with the anchorage value of teeth.[8] Therefore, the PDL_Area is important in predicting periodontal support and orthodontic tooth movement.

Previous scholars used various methods to measure the root surface area (RSA) below the cementoenamel junction (CEJ). However, these methods have disadvantages; for instance, these methods lack accuracy and precision and require difficult procedures, such as tooth extraction.[9] Researchers reconstructed root surfaces on the basis of microcomputed tomography (micro-CT) or cone-beam computed tomography (CBCT) to detect apical root resorption cavities[10,11] and measured RSA as an important marker for determining the periodontal treatment plan and prognosis of the teeth.[6] However, RSA measurements do not consider alveolar bone conditions; in recent years, the PDL surface area, or alveolar bone-attached root surface, has been studied to evaluate the periodontal health of teeth. Researchers artificially simulated the PDL_Area in digital tooth models in vitro.[6,12-15] To date, no previous study has performed periodontal attachment level-based 3-dimensional (3D) PDL_Area measurements in humans in vivo.

The method of measuring alveolar bone thickness and the vertical bone level (VBL) of patients with Class III malocclusion in the sagittal plane of CBCT images has been well established.[1,2,16-18] During presurgical orthodontic treatment, mandibular incisors have shown a significant reduction in the VBL and bone thickness and gingival recession[17-19]; the alveolar bone at the lingual surface of mandibular incisors may be more vulnerable to dentoalveolar decompensation.[19] Past studies of periodontal damage during surgical orthodontic treatment of patients with Class III malocclusion have had several limitations. Studies have focused primarily on measuring the height and thickness of alveolar bone at the labial and lingual surfaces of incisors in the sagittal plane. Evaluating these 2-dimensional (2D) measurements without considering the 3D PDL_Area may not adequately indicate the severity of periodontal lesions. Moreover, 2D linear measurements describe VBLs in a 1-dimensional way without taking the root shape change into account; this approach underestimates the amount of true periodontium loss.[12,13,20] Because of the limited choice of measurement plane, few studies have considered the effect of vertical bone loss at the proximal surfaces of incisors,[18] which may have introduced potential bias in evaluating the surrounding alveolar bone. Finally, many studies did not consider postsurgical orthodontic treatment, whereas periodontal damage may have occurred during this period and would differ from presurgical orthodontic treatment.

CBCT 3D reconstruction has been confirmed to be an accurate, reliable, nondestructive method to visualize the anatomic structure of teeth[10,21,22] and periodontal bone defects.[23] Instead of artificially simulating periodontal attachment levels in vitro, we measured RSA and PDL_Area in vivo using the CBCT 3D reconstruction method; acquiring these measurements with this method allowed periodontal and endodontic conditions to be assessed more thoroughly and comprehensively. In addition, by evaluating the VBLs of 4 surfaces around incisors, we can investigate the differences in alveolar bone levels among surfaces; these differences can provide insight into the causal relationship between the morphology of periodontal deterioration and orthodontic tooth movement.

This study aimed to investigate periodontal defects during the surgical orthodontic treatment of patients with high-angle Class III malocclusion by measuring RSA, PDL_Area, and VBLs around the maxillary and mandibular central incisors after CBCT 3D reconstruction.

MATERIAL AND METHODS

Selection of the sample

This retrospective study was approved by the Biomedical Ethics Committee of Peking University School and Hospital of Stomatology (PKUSSIRB-201951168). Thirty patients with Class III malocclusion (15 men, 15 women; mean age, 20.53 ± 2.86 years) were treated at the Department of Orthodontics at Peking University Hospital of Stomatology from 2013 to 2019 were enrolled (Table I). All subjects underwent bilateral sagittal split ramus osteotomy and LeFort I surgery with rigid internal fixation and presurgical and postsurgical orthodontic treatment. The sample size calculation was determined by power analysis and sample size software (version 15.0; NCSS, Kaysville, Utah) on the basis of vertical bone loss of a lower limit of 95% confidence interval (LCIs).[17] A minimum sample size of 30 subjects was required to conduct a

Table I. Patient characteristics in this study

Characteristics	*Male (n = 15)*	*Female (n = 15)*
Age, y	19.69 ± 3.38	21.06 ± 2.69
T0-T1, mo	24.56 ± 4.49	25.86 ± 5.84
T1-T2, mo	11.50 ± 4.96	11.53 ± 4.95
T0-T2, mo	36.06 ± 6.90	37.40 ± 7.07

Note. Presented values are mean ± standard deviation.

statistical analysis with a significance level of 0.05 and a statistical power of 80%.

Inclusion criteria were as follows: aged >18 years; skeletal and dental Class III malocclusion (ANB <0°; overjet <0 mm), high angle (SN-MP >37.7°), mild crowding (<4 mm) in the maxillary and mandibular arch, bilateral first premolar extraction in the maxillary arch, and no extraction in the mandibular arch.

The exclusion criteria were severe facial asymmetry (>3 mm of chin point deviation from the facial midline), noticeable periodontal disease, cleft lip or palate or other craniofacial syndromes, missing or decayed teeth before treatment (except for the third molars), and orthodontic treatment history.

All the orthodontic treatment was performed by a single orthodontist (X.L) with a straight-wire fixed appliance (0.022-in slot size, MBT prescription), and the archwire sequence involved 0.014, 0.016, 0.018, and 0.018 × 0.025-in nickel-titanium wires followed by a 0.018 × 0.025-in stainless-steel wire. During presurgical orthodontic treatment, anchorage in the maxillary arch was reinforced using miniscrew implants, and an upper limit of 95% confidence interval (UCIs) could move in a controlled tipping manner.

Large field-of-view (FOV) CBCT imaging using NewTom VG (Aperio Services, Verona, Italy) was performed before treatment (T0), after presurgical orthodontic treatment (T1), and after treatment (T2). In addition, lateral cephalograms were reconstructed from CBCT images. CBCT images were recorded in full scan mode (110 kVp; 2.05 mA; 0.3-mm voxel size; scan time, 3.6 seconds; and FOV of 15 × 12 cm).

UCIs and LCIs on the right side were selected as subjects for measurement. The definitions of the measurements used in this study are described in Table II.

Measurement of VBLs

CBCT data in digital imaging and communication in medicine format were imported into Dolphin 11.8 (Dolphin Imaging and Management Solutions, Chatsworth, Calif).

The orientation of CBCT images used in this study was modified from previous reports.[16,17] Measurements were acquired from sagittal slices of CBCT images in which incisors were the widest labiolingually in the axial view, and the long axis of the root was adjusted to the vertical orientation to obtain the axial, coronal, and sagittal root planes (Fig 1). The 2D root length was determined in the sagittal plane by connecting the root apex and the midpoint of the CEJ. The vertical linear distance between the CEJ and the incisor alveolar bone crests was measured as the VBL. The corresponding distances were obtained for the mesial VBL (MBL), distal VBL (DBL), labial VBL (LABL), and lingual VBL (LBL).

Table II. Definitions of measurements used in this study

Measurements	*Definitions*
RSA, mm^2	The whole root surface area up to the CEJ
PDL_Area, mm^2	The part of the RSA that is covered by PDL and alveolar bone
Root resorption, mm^2	The reduction amount of RSAs between 2 time points
Bone loss, mm^2	The PDL_Area loss caused by vertical bone loss; the reduction amount of PDL_Areas between 2 time points minus root resorption during 2 time points
Root length, mm	Distance from the midpoint of CEJ on the labial and lingual side to the root apex of maxillary or mandibular incisors
MBL, mm	Vertical bone loss on the mesial side of maxillary or mandibular incisors; distance from CEJ to alveolar crest on the mesial side parallel to root length
DBL, mm	Vertical bone loss on the distal side of maxillary or mandibular incisor; distance from CEJ to alveolar crest on the distal side parallel to root length
LABL, mm	Vertical bone loss on the labial side of maxillary or mandibular incisor; distance from CEJ to alveolar crest on the labial side parallel to root length
LBL, mm	Vertical bone loss on the lingual side of maxillary or mandibular incisor; distance from CEJ to alveolar crest on the lingual side parallel to root length

RSA and PDL area measurements

Digital imaging and communication in medicine files were imported into Mimics software (version 19; Materialise, Leuven, Belgium). We then reconstructed 3D digital tooth and bone in vivo models with Mimics. The tooth was segmented first. CBCT images in Mimics had predefined thresholds (minimum, 1200 segments; maximum, 3071 segments) that correspond to tooth density and the designated area for 3D reconstructions (Fig 2, *A*). The tooth, PDL, and jawbone were assembled

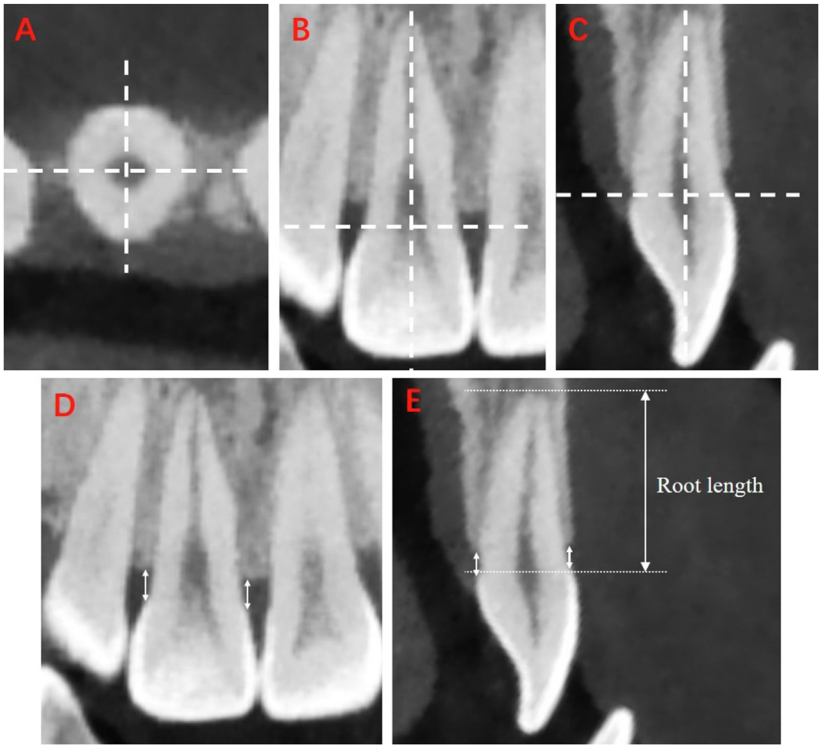

Fig 1. Example and illustrations of VBL measurement around UCIs and LCIs: **A-C,** Example of CBCT images of the maxillary right central incisor. The orientation of axial, coronal, and sagittal slices; **D** and **E,** The measurements of VBLs and root length.

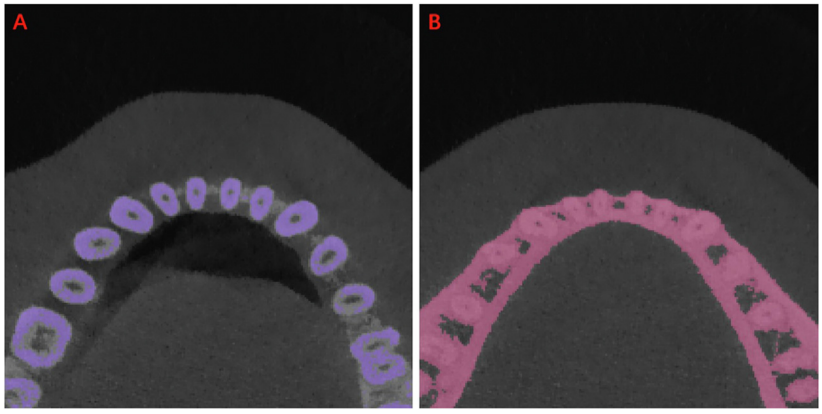

Fig 2. Process of segmenting tooth and alveolar bone in Mimics: **A,** Thresholding mask based on tooth density; **B,** Thresholding mask based on the general bone value.

to create the digital bone model (Fig 2, *B*). In each CBCT slide, manual refinement was conducted through a 2D slide-by-slide procedure to modify the primary tooth gray scale images.[24] The digital tooth and bone models were exported in stereolithography file format.

The corresponding stereolithography images of the tooth and bone models at T0, T1, and T2 were imported into Geomagic software (Geomagic, Cary, NC) (Fig 3, *A*). To obtain the RSA model, the tooth model was separated into 2 parts along the CEJ curve, and the crown was

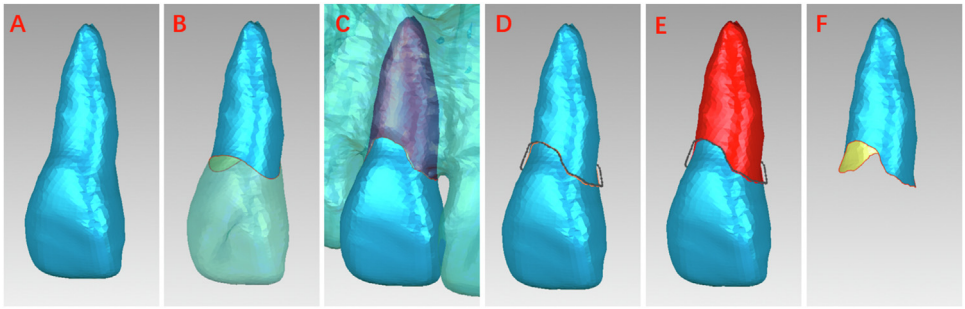

Fig 3. Separation of RSA and PDL_Area: **A,** 3D digital tooth model generated from CBCT; **B,** The model was separated along the CEJ curve, and RSA was obtained; **C,** The periodontal alveolar attachment level was drawn around the incisors on the bone model; **D,** The curve on the bone model was projected to the tooth model; **E,** The tooth model was separated along the periodontal alveolar attachment curve, and the PDL was obtained; **F,** The crown was removed, and PDL was preserved.

removed (Fig 3, *B*). To obtain the PDL_Area model, we identified and drew points along the periodontal attachment level around the incisors on the digital bone model, and a curve was generated by connecting the points marked on the model surface using the creation method in Geomagic (Fig 3, *C*). The created boundary curve was projected to the digital tooth model (Fig 3, *D*), the model was separated along the curve into 2 parts, and the PDL_Area model was preserved (Fig 3, *E*).

Statistical analysis

Statistical analyses were performed using SPSS (version 20.0; IBM Corp, Armonk, NY). All measurements were taken twice at an interval of 2 weeks by the same investigator. The average of these 2 measurements was used for statistical analysis. Furthermore, measurements of 20 randomly chosen subjects were taken by 2 blinded authors (H.L and H.M, who have between 4 and 8 years of experience in dental and periodontal imaging). The systematic intraexaminer error was determined using paired t test. Intraexaminer and interexaminer agreements were calculated using the intraclass correlation coefficient (ICC).

Furthermore, the error in the segmenting process was evaluated by measuring the total surface area of the teeth. The segmenting error was analyzed with the Bland-Altman test. Analysis of variance with the general linear model was used to analyze changes in VBL, RSA, PDL_Area, and repeated measurements. Bonferroni correction was applied to compensate for multiple comparisons.

One-way analysis of variance with Duncan's multiple comparison test was performed to compare VBLs on different surfaces. The Mann-Whitney U test was used to compare the bone loss and root resorption of different teeth.

RESULTS

Change in PDL area and RSA of UCIs and LCIs during surgical orthodontic treatment

The PDL_Area of UCIs and LCIs decreased significantly during pre- and postsurgical orthodontic treatment (Table III) (Fig 4). From T0 to T2, the PDL_Area of UCIs and LCIs decreased to 28.39 ± 21.94 mm^2 and 41.35 ± 14.89 mm^2 (Table IV), respectively, and LCIs indicated greater PDL_Area loss than UCIs (P <0.05). At T2, the PDL_Area was reduced by 21.13 ± 16.48% for UCIs and 38.64 ± 13.39% for LCIs compared with T0 (Table IV).

The RSA and root length of UCIs and LCIs decreased significantly between T0 and T1 and between T1 and T2, which suggests that root resorption occurs continuously over the treatment course (Table III) (Fig 4). Moreover, the root resorption of UCIs and LCIs had no apparent difference from T0 to T1, T1 to T2, and T0 to T2. At T2, RSA was reduced by 10.56 ± 9.14% for UCIs and 11.30 ± 7.65% for LCIs compared with that at T0 (Table IV).

As shown in Table V, from T0 to T1, there was no difference between root resorption and bone loss, but from T1 to T2, root resorption was significantly greater than bone loss for UCIs. From T0-T2, there was no apparent difference between root resorption and bone loss.

For LCIs, from T0 to T1, bone loss was significantly greater than root resorption, but from T1 to T2, there was no statistically significant difference between bone loss and root resorption. From T0 to T2, the bone loss was significantly greater than root resorption.

From T0 to T1 and from T0 to T2, the bone loss of LCIs was significantly greater than that of UCIs, but from T1 to T2, there was no apparent difference in bone loss between UCIs and LCIs. The results suggest greater periodontal damage of LCIs compared with

Table III. Comparison of PDL_Area and RSA of maxillary and mandibular central incisors during surgical orthodontic treatment

Measurement	*T0 stage*	*T1 stage*	*T2 stage*	P *value*[†]	*Multiple comparisons*[‡]
UCI					
PDL_Area, mm^2	137.41 ± 27.00	117.16 ± 31.30	109.02 ± 33.24	<0.001**	T0>T1>T2
RSA, mm^2	155.15 ± 27.21	146.22 ± 28.56	138.82 ± 27.25	<0.001**	T0>T1>T2
Root length, mm	11.17 ± 2.04	10.19 ± 2.17	9.82 ± 2.28	<0.001**	T0>T1>T2
LCI					
PDL_Area, mm^2	108.01 ± 18.19	79.72 ± 23.93	66.66 ± 20.34	<0.001**	T0>T1>T2
RSA, mm^2	125.53 ± 15.09	118.63 ± 16.01	111.24 ± 16.12	<0.001**	T0>T1>T2
Root length, mm	11.06 ± 0.95	10.32 ± 1.10	9.96 ± 1.05	<0.001**	T0>T1>T2

Note. Presented values are mean ± standard deviation.
**$P \leq 0.01$; [†]One-way repeated measures analysis was performed to compare T0, T1, and T2; [‡]Multiple comparisons: Bonferroni test with repeated measures analysis.

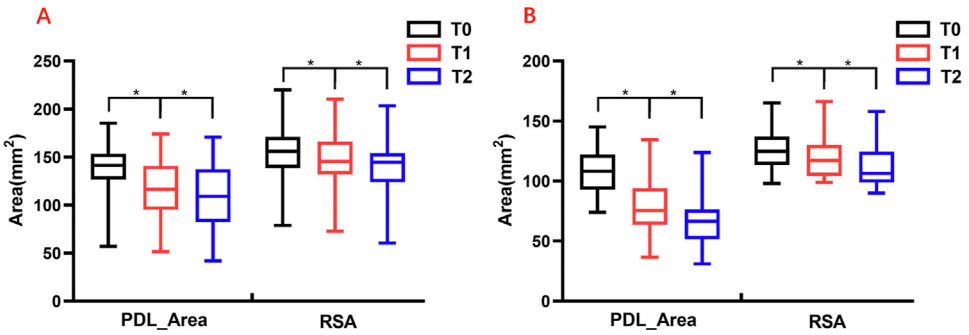

Fig 4. The boxplots of PDL_Area and RSA: **A,** Comparison of PDL_Area and RSA of UCIs during surgical orthodontic treatment; **B,** Comparison of PDL_Area and RSA of LCIs during surgical orthodontic treatment. *$P \leq 0.05$; **$P \leq 0.01$.

Table IV. Changing amount and percentage of PDL_Area, RSA, and root length in T1-T0, T2-T1, and T2-T0

	UCI		*LCI*		
Measurement	*Mean (% change)*	*Standard deviation (% change)*	*Mean (% change)*	*Standard deviation (% change)*	P *value*[†]
PDL_Area, mm^2					
T1-T0	−20.25 (−15.15)	17.5 (12.91)	−28.29 (−26.67)	16.73 (15.57)	0.08
T2-T1	−8.14 (−5.98)	12.76 (10.18)	−13.06 (−11.97)	12.74 (10.64)	0.15
T2-T0	−28.39 (−21.13)	21.94 (16.48)	−41.35 (−38.64)	14.89 (13.39)	0.011*
RSA, mm^2					
T1-T0	−8.93 (−5.73)	13.62 (8.86)	−6.90 (−5.40)	8.37 (6.68)	0.51
T2-T1	−7.40 (−4.83)	10.88 (7.12)	−7.39 (−5.90)	9.87 (7.81)	0.99
T2-T0	−16.33 (−10.56)	13.68 (9.14)	−14.29 (−11.30)	10.06 (7.65)	0.52
Root length, mm					
T1-T0	−0.98 (−9.49)	1.08 (10.38)	−0.74 (−6.54)	0.67 (5.92)	0.22
T2-T1	−0.37 (−4.01)	0.51 (4.67)	−0.36 (−3.29)	0.40 (3.59)	0.67
T2-T0	−1.35 (−13.51)	1.26 (11.58)	−1.10 (−9.83)	0.75 (6.56)	0.21

*$P \leq 0.05$; [†]A matched *t* test was performed to compare the difference in changing amounts between UCIs and LCIs. The percentage of changing amount compared with T0 is presented in parentheses.

Table V. Comparison of root resorption and bone loss in T1-T0, T2-T1, and T2-T0

	Root resorption, mm²		*Bone loss, mm²*		
Comparisons	*Median*	*Quartile*	*Median*	*Quartile*	P *value*[†]
T1-T0					
UCI	9.42	0.50	9.45	0.88	0.70
LCI	5.72	0.15	20.82	10.43	<0.01**
P value[‡]	0.44		0.008**		
T2-T1					
UCI	7.30	1.47	1.24	0.02	0.02*
LCI	5.65	0.04	3.95	0.07	0.43
P value[‡]	0.87		0.23		
T2-T0					
UCI	19.44	8.20	7.49	0.72	0.22
LCI	15.77	6.82	27.89	16.36	0.001**
P value[‡]	0.22		0.002**		

*$P \leq 0.05$; **$P \leq 0.01$; [†]Mann-Whitney U test was performed to compare the differences between root resorption and bone loss; [‡]Mann-Whitney U test was performed to compare the difference between UCIs and LCIs.

UCIs in presurgical orthodontic treatment. To explore the alveolar periodontal damage around the incisors, MBL, DBL, LABL, and LBL were measured.

Change in VBLs of UCIs and LCIs during surgical orthodontic treatment

As shown in Table VI, at T0, the mean VBLs around UCIs were <2 mm except for the MBL, and the LBL was 1.38 mm, which was small compared with the VBLs of other surfaces. For LCIs, VBLs were >2 mm, and VBLs of proximal sites were small than those of labial and lingual surfaces.

For UCIs, between T0 and T1, the LBL increased significantly from 1.38 mm to 3.56 mm ($P < 0.05$), whereas there was no apparent change in the LBL between T1 and T2. LABL, MBL, and DBL values did not change significantly from T0 to T2. For LCIs, MBL, LABL, and LBL values increased significantly ($P < 0.01$) from T0 to T1, whereas the DBL showed no apparent change. In addition, the LABL increased significantly from T1 to T2 ($P < 0.05$), whereas MBL, DBL, and LBL showed no apparent change.

The mean amounts of change in VBL from T0 to T2 at different surfaces of UCIs and LCIs are shown in Table VII. During the treatment course, the LBL of UCIs increased by 2.22 ± 2.30 mm, which was significantly greater than the increase observed in labial and proximal surfaces. For LCIs, LABL and LBL values increased by 3.06 ± 2.50 mm and 3.40 ± 2.39 mm, respectively, statistically greater than the changes observed at proximal surfaces.

Changes in the proximal surfaces of UCIs and LCIs showed no apparent difference. The results suggest that the VBL of the labial surface of UCIs and proximal surfaces of UCIs and LCIs are relatively stable compared with the VBL of other surfaces during surgical orthodontic treatment.

The root length of UCIs and LCIs decreased significantly during the treatment (Table III), but the mean change in root length between T0 and T2 was <2 mm.

Intra- and interexaminer agreements

We found a very high agreement within and between examiners. Systematic intraexaminer error was evaluated at $P < 0.05$ and was found to be statistically insignificant. In addition, strong intraexaminer reliability (ICC, 0.985; 95% confidence interval [CI], 0.973-0.991) was found. Differences between examiners were also analyzed, and the results showed high interexaminer agreement for tooth segmentation (ICC, 0.992; 95% CI, 0.980-0.997) and (ICC, 0.947; 95% CI, 0.871-0.979) for PDL_Area measurement). Moreover, the Bland-Altman analysis showed good consistency between 2 examiners in segmenting and PDL_Area measuring.

DISCUSSION

This study focuses mainly on quantifying the alveolar bone condition of UCIs and LCIs. These factors are essential for diagnosing patients with high-angle Class III malocclusion undergoing surgical orthodontic treatment.

In this study, we found that during surgical orthodontic treatment, the PDL_Area of UCIs and LCIs decreased continuously in presurgical and postsurgical orthodontic treatment. After debonding, the percentages of PDL_Area loss of UCIs and LCIs were 21.13% and 38.64%, respectively, and LCIs showed significantly more PDL loss than UCIs. According to the 2018 classification of periodontal diseases and conditions,[25] mild periodontal support bone loss is characterized by 16%-30% radiographic VBL loss; moderate periodontal support involves a VBL loss >30% in root length but still <50% overall. A previous study performed by Hong et al[12] investigated 3D RSA and periodontal attachment levels of single-root premolars. They reported that at the 15% coronal 2D root length level, the 3D RSA apical to the CEJ was 21%, and at the 30% coronal 2D root length level, the 3D RSA apical to the CEJ was approximately 40%.[12] Although morphologic characteristics differ between single-root premolars and incisors, their report provided a 3D reference

Table VI. Comparison of VBLs of UCIs and LCIs during surgical orthodontic treatment

Measurement, mm	*T0 stage*	*T1 stage*	*T2 stage*	P *value*[†]	*Multiple comparisons*[‡]
UCI					
MBL	2.39 ± 0.93	2.51 ± 0.92	2.32 ± 0.84	0.61	–
DBL	1.75 ± 0.54	1.86 ± 0.66	1.9 ± 0.51	0.44	–
LABL	1.79 ± 0.63	2.09 ± 1.26	2.01 ± 0.71	0.22	–
LBL	1.38 ± 0.51	3.56 ± 2.11	3.59 ± 2.17	<0.001**	T0 < T1, T2
LCI					
MBL	2.12 ± 0.4	2.4 ± 0.56	2.35 ± 0.45	0.01*	T0 < T1, T2
DBL	2.07 ± 0.53	2.28 ± 0.58	2.32 ± 0.47	0.02*	T0, T1 < T1, T2
LABL	2.53 ± 1.57	4.16 ± 2.72	5.59 ± 2.52	<0.01**	T0 < T1 < T2
LBL	2.30 ± 1.36	5.28 ± 2.58	5.70 ± 2.52	<0.01**	T0 < T1, T2

*$P \leq 0.05$; **$P \leq 0.01$; [†]One-way repeated measures analysis was performed to compare T0, T1, and T2; [‡]Bonferroni test with repeated measures analysis.

Table VII. Comparison of the change of VBLs (T2-T0) of UCIs and LCIs

Comparison	*ΔMBL, mm*	*ΔDBL, mm*	*ΔLABL, mm*	*ΔLBL, mm*	P *value*[†]	*Multiple comparison*
UCI	0.07 ± 1.05	−0.15 ± 0.62	−0.23 ± 0.54	−2.22 ± 2.30	<0.001**	L > M, D, LA
LCI	−0.24 ± 0.44	−0.25 ± 0.45	−3.06 ± 2.50	−3.40 ± 2.39	<0.001**	LA, L > M, D
P value[‡]	0.18	0.25	<0.001**	0.31		

Note. Presented values are mean ± standard deviation.
*$P \leq 0.05$; **$P \leq 0.01$; [†]Analysis of variance was performed for comparison between different surfaces; [‡]Matched *t* test was performed to compare the difference between UCIs and LCIs.

regarding the severity of periodontal damage for this study.

The RSA of UCIs and LCIs decreased continuously in the treatment course in this study, which means that root resorption occurred in both the presurgical and postsurgical orthodontic courses. Many studies have considered the effect of root resorption on periodontal support, and the evaluation of linear measurements of VBLs without considering root length and root shape tends to underestimate the periodontal support loss.[7,20] However, no previous studies have attempted to obtain the exact values of the PDL_Area loss caused by root resorption or VBL loss, and no comparison between root resorption and bone loss has been performed. This study is the first to implement this type of comparison. We found no difference in RSA measurements for UCIs and LCIs in presurgical and postsurgical orthodontic treatment periods; this lack of change demonstrates that the periodontal support loss caused by root resorption for UCIs and LCIs is statistically the same. In the presurgical orthodontic treatment period for LCIs, VBL loss played a dominant role in PDL_Area loss compared with root resorption. The PDL_Area loss caused by VBL loss in LCIs was significantly greater than that in UCIs. The results emphasize the high risk of alveolar bone recession of LCIs in decompensation treatment and its impact on periodontal support. In the postsurgical orthodontic treatment period for LCIs, there was no difference between PDL_Area loss caused by VBL loss or root resorption. For UCIs, VBL loss and root resorption had the same effect on PDL_Area loss during the entire treatment course. The results provide insight into the effect of root resorption during orthodontic treatment for clinicians, and root resorption leads to not only endodontic damage but also periodontal support loss. Hence, it is necessary to consider root resorption when evaluating periodontal damage during surgical orthodontic treatment for patients with high-angle skeletal Class III malocclusion. Nevertheless, during the presurgical treatment period, root resorption is less critical in its effects on periodontal support loss than an alveolar bone recession for LCIs.

To investigate the exact PDL_Area loss occurring at various surfaces around incisors, MBLs, DBLs, LABL, and LBLs were measured in Dolphin Imaging software. We found that most of the VBL losses occurred at the presurgical orthodontic stage, and deterioration in postsurgical orthodontics, such as that observed at the lingual surface of UCIs, was not significant. The results were in accord with previous studies.[17] However, the labial surface of LCIs had a significant reduction in VBL in both presurgical and postsurgical

orthodontic treatment. This was expected because for patients with high-angle skeletal Class III malocclusion, before treatment, vertical bone loss is more severe in LCIs than in UCIs, and the alveolar bone width of LCIs is significantly thinner than that of UCIs.[1,16] Moreover, the proclination of LCIs for decompensation and adjustment of detailed occlusion in postsurgical orthodontic treatment seems to promote labial alveolar bone recession. The retrolination movement of UCIs in presurgical orthodontic treatment may result in a lingual bone level reduction.[26] Our previous study[26] reported that during the presurgical orthodontic course, the edges of UCIs and LCIs extruded vertically; however, the extrusion movement was relatively insignificant compared with the vertical position before treatment. In this study, we emphasized the change in periodontal condition around the anterior incisors during the treatment course.

We compared the change in VBLs from T0 to T2 at different UCIs and LCIs, and the results indicated that the change in VBL at the lingual surface of UCIs was significantly greater than that at the labial and proximal surfaces. Although VBLs at proximal surfaces of LCIs showed a significant reduction during the treatment course, the change in VBLs at the labial and lingual surfaces of LCIs was strikingly greater than the change at proximal surfaces. Previous studies simulated VBL recession in vitro and assumed that the alveolar bone height losses around the incisors at different surfaces were equal.[6,12-15] However, our results indicate that for UCIs and LCIs of patients with high-angle Class III malocclusion who underwent surgical orthodontic treatment, the deterioration of periodontal alveolar bone is not pure horizontal bone loss, and VBLs at proximal surfaces are relatively preserved compared with labial and lingual surfaces. After debonding, 3 wall intrabony pockets are discernible for the coronal part of the UCIs in which labial surfaces are intact and both proximal walls.[27] For LCIs, the proximal walls are intact, but the labial and lingual walls have been destroyed. Augmented corticotomy could be used to maintain the labial bone volume,[28] which may improve the periodontal prognosis of LCIs.

Previous studies have found that the 3D measurement of RSA of periodontal attachment and 2D VBL is inconsistent,[13] and diagnosis on the basis of the condition of the 2D radiographic bone and clinical attachment losses without considering 3D RSA is potentially inadequate and may underestimate the severity of periodontal damage.[12] Therefore, PDL_Area measurements are considered suitable to indicate the severity of periodontal deterioration during the orthodontic treatment course. Researchers have simulated the PDL_Area in vitro by marking cutting lines parallel to the CEJ curve on the surface of digital tooth models.[6,12-15] However, in clinical practice, the alveolar bone around the teeth is typically not reduced equally at various sites during surgical orthodontic treatment of patients with high-angle skeletal Class III malocclusion. In addition, in vitro simulations do not reflect periodontal morphology changes during treatment. Moreover, the in vitro simulation of the cross-sectional study did not consider the impact of root resorption on periodontal support. This study is the first to measure PDL_Area by producing 3D models of teeth and alveolar bone using CBCT 3D reconstructions in vivo, which can better reflect the clinical situation.

CBCT provides accurate and reproducible 3D reconstructions of the teeth that can be useful for some clinical applications compared with micro-CT,[10,29] and some researchers reported that a voxel size of 0.30 mm would be suitable for accurate tooth segmentation.[21,22,30,31] Jia et al[32] compared single-root teeth RSA measurement in a sheep in situ on the basis of CBCT data and images from an optical scanner and found that RSA data obtained from CBCT with different FOVs (12 × 8 cm or 8 × 8 cm) and voxel sizes (0.15 mm or 0.30 mm) were as accurate as optical scanner measurements taken ex vivo.

Regarding periodontal bone loss assessment, CBCT provides very high agreement regarding intrabony volumetric measurement of periodontal defects compared with micro-CT in vitro regardless of the voxel size.[23] Compared with intrasurgical measurements of vertical or horizontal bone loss, CBCT showed a corresponding measurement[33] or underestimation[34] of vertical or horizontal bone loss, with accuracy between 58% and 93%.[35] However, Patcas et al[36] reported that it is difficult to accurately measure the boundary of thin alveolar bone with CBCT even with the 0.125-mm voxel protocol, and there is a risk of overestimating fenestrations and dehiscences. Various factors of CBCT exposure parameters may influence image quality, such as FOV size and voxel thickness.[37,38] The differences in CBCT exposure parameters between studies may explain the divergence in conclusions. In this study, because of the limited CBCT resolution, 2 evaluators (H.L. and H.M.) knowledgeable about dental and periodontal morphology were asked to identify the periodontal attachment level to improve measurement accuracy and consistency.

Currently, accurate 3D measurements require high-resolution images, and micro-CT can reach a spatial resolution of 15-18 μm, whereas the resolution of CBCT is lower.[29] Nevertheless, CBCT subjects are exposed to a higher radiation dose than conventional x-ray images.[39] Therefore, each time CBCT is used, the potential harm must be carefully weighed against the potential benefit

according to the as low as reasonably achievable principles. In addition, smaller voxel sizes are usually linked to increased imaging exposure time and ionizing radiation concomitantly. The CBCT scans used in this retrospective study were acquired routinely in our facility for research and clinical purposes at T0, T1, and T2; these images were not taken at the highest resolution in the interest of patient safety and to keep exposure levels as low as diagnostically acceptable. A large FOV at different time points provided important diagnostic information for orthognathic surgeons, periodontal clinicians, and orthodontists. However, we believe the scan data are sufficient to allow scientifically valid analysis and conclusions. To test the interexaminer reliability, 20 randomly chosen subjects were measured by 2 blinded and calibrated authors (H.L. and H.M.) in this retrospective study. However, it was difficult to follow the blind method in the material collection and data measurement; thus, the limitation should not be ignored.

Furthermore, we delineated the periodontal attachment level around the incisors to obtain a PDL_Area model and measured VBLs at different surfaces; these VBL measurements mainly focused on the morphologic characteristics of alveolar dehiscence rather than fenestration. Even with the limitations mentioned above, the results signify, and reiterate to clinicians, the periodontal risk of patients with high-angle Class III malocclusion in surgical orthodontic treatment and guide augmented corticotomy performance. In addition, the 3D tooth models used in this study were saved from being used for sectional area measurements and as research material for future studies.

CONCLUSIONS

In this study, we found that for patients with high-angle Class III malocclusion undergoing surgical orthodontic treatment, the periodontal support of UCIs and LCIs decreased continuously during presurgical and postsurgical orthodontic treatment. LCIs may be more vulnerable to dentoalveolar decompensation than UCIs. VBLs of the labial surface of UCIs and proximal surfaces of UCIs and LCIs are relatively preserved compared with VBLs of other surfaces. The effect of root resorption on periodontal support should not be ignored. Thus, the CBCT 3D reconstruction method provides useful information for clinicians to evaluate periodontal prognosis and determine an appropriate treatment plan.

AUTHOR CREDIT STATEMENT

Hangmiao Lyu contributed to conceptualization, data curation, and original manuscript preparation; Huimin Ma contributed data curation, formal analysis, and visualization; Jianxia Hou contributed to resources; Xiaoxia Wang contributed to resources; Yong Wang contributed to methodology; Yijiao Zhao contributed methodology; and Xiaotong Li contributed to supervision and manuscript review and editing.

REFERENCES

1. Kook YA, Kim G, Kim Y. Comparison of alveolar bone loss around incisors in normal occlusion samples and surgical skeletal Class III patients. Angle Orthod 2012;82:645-52.
2. Lee S, Hwang S, Jang W, Choi YJ, Chung CJ, Kim KH. Assessment of lower incisor alveolar bone width using cone-beam computed tomography images in skeletal Class III adults of different vertical patterns. Korean J Orthod 2018;48:349-56.
3. Beertsen W, McCulloch CA, Sodek J. The periodontal ligament: a unique, multifunctional connective tissue. Periodontol 2000 1997;13:20-40.
4. de Jong T, Bakker AD, Everts V, Smit TH. The intricate anatomy of the periodontal ligament and its development: lessons for periodontal regeneration. J Periodontal Res 2017;52:965-74.
5. Jiang N, Guo W, Chen M, Zheng Y, Zhou J, Kim SG, et al. Periodontal ligament and alveolar bone in health and adaptation: tooth movement. Front Oral Biol 2016;18:1-8.
6. Park SB, An SY, Han WJ, Park JT. Three-dimensional measurement of periodontal surface area for quantifying inflammatory burden. J Periodontal Implant Sci 2017;47:154-64.
7. Kalkwarf KL, Krejci RF, Pao YC. Effect of apical root resorption on periodontal support. J Prosthet Dent 1986;56:317-9.
8. Proffit WR. The biologic basis of orthodontic therapy. In: Proffit W, Fields HW, editors. Contemporary Orthodontics. 6th ed. Philadelphia: Elsevier; 2018. p. 265-6.
9. Hujoel PP. A meta-analysis of normal ranges for root surface areas of the permanent dentition. J Clin Periodontol 1994;21:225-9.
10. Wang Y, He S, Guo Y, Wang S, Chen S. Accuracy of volumetric measurement of simulated root resorption lacunas based on cone beam computed tomography. Orthod Craniofac Res 2013;16:169-76.
11. Zhong J, Chen J, Weinkamer R, Darendeliler MA, Swain MV, Sue A, et al. In vivo effects of different orthodontic loading on root resorption and correlation with mechanobiological stimulus in periodontal ligament. J R Soc Interface 2019;16:20190108.
12. Hong HH, Hong A, Huang YF, Liu HL. Incompatible amount of 3-D and 2-D periodontal attachments on micro-CT scanned premolars. PLoS One 2018;13:e0193894.
13. Hong HH, Chang CC, Hong A, Liu HL, Wang YL, Chang SH, et al. Decreased amount of supporting alveolar bone at single-rooted premolars is under estimated by 2D examinations. Sci Rep 2017;7:45774.
14. Gu Y, Tang Y, Zhu Q, Feng X. Measurement of root surface area of permanent teeth with root variations in a Chinese population-A micro-CT analysis. Arch Oral Biol 2016;63:75-81.
15. Gu Y, Zhu Q, Tang Y, Zhang Y, Feng X. Measurement of root surface area of permanent teeth in a Chinese population. Arch Oral Biol 2017;81:26-30.
16. Kim Y, Park JU, Kook YA. Alveolar bone loss around incisors in surgical skeletal Class III patients. Angle Orthod 2009;79:676-82.
17. Lee KM, Kim YI, Park SB, Son WS. Alveolar bone loss around lower incisors during surgical orthodontic treatment in mandibular prognathism. Angle Orthod 2012;82:637-44.

18. Choi YJ, Chung CJ, Kim KH. Periodontal consequences of mandibular incisor proclination during presurgical orthodontic treatment in Class III malocclusion patients. Angle Orthod 2015;85:427-33.
19. Sun B, Tang J, Xiao P, Ding Y. Presurgical orthodontic decompensation alters alveolar bone condition around mandibular incisors in adults with skeletal Class III malocclusion. Int J Clin Exp Med 2015; 8:12866-73.
20. Klock KS, Gjerdet NR, Haugejorden O. Periodontal attachment loss assessed by linear and area measurements in vitro. J Clin Periodontol 1993;20:443-7.
21. Liu Y, Olszewski R, Alexandroni ES, Enciso R, Xu T, Mah JK. The validity of in vivo tooth volume determinations from cone-beam computed tomography. Angle Orthod 2010;80:160-6.
22. Wang C, Liu Y, Wang S, Wang Y, Zhao Y. Evaluation of in vivo digital root reconstruction based on anatomical characteristics of the periodontal ligament using cone beam computed tomography. Sci Rep 2018;8:269.
23. Tayman MA, Kamburoğlu K, Küçük Ö, Ateş FSÖ, Günhan M. Comparison of linear and volumetric measurements obtained from periodontal defects by using cone beam-CT and micro-CT: an in vitro study. Clin Oral Investig 2019;23:2235-44.
24. Forst D, Nijjar S, Flores-Mir C, Carey J, Secanell M, Lagravere M. Comparison of in vivo 3D cone-beam computed tomography tooth volume measurement protocols. Prog Orthod 2014;15:69.
25. Papapanou PN, Sanz M, Buduneli N, Dietrich T, Feres M, Fine DH, et al. Periodontitis: consensus report of workgroup 2 of the 2017 World Workshop on the Classification of Periodontal and Peri-Implant Diseases and Conditions. J Periodontol 2018;89(Suppl 1):S173-82.
26. Ma H, Li W, Xu L, Hou J, Wang X, Ding S, et al. Morphometric evaluation of the alveolar bone around central incisors during surgical orthodontic treatment of high-angle skeletal Class III malocclusion. Orthod Craniofac Res 2021;24:87-95.
27. Watkin A. The intrabony pocket—classification and therapy. Diastema 1970;3:15-7.
28. Soltani L, Loomer PM, Chaar EE. A novel approach in periodontally accelerated osteogenic orthodontics (PAOO): a case report. Clin Adv Periodontics 2019;9:110-4.
29. Al-Rawi B, Hassan B, Vandenberge B, Jacobs R. Accuracy assessment of three-dimensional surface reconstructions of teeth from cone beam computed tomography scans. J Oral Rehabil 2010; 37:352-8.
30. Sang YH, Hu HC, Lu SH, Wu YW, Li WR, Tang ZH. Accuracy assessment of three-dimensional surface reconstructions of in vivo teeth from cone-beam computed tomography. Chin Med J (Engl) 2016; 129:1464-70.
31. Ahlbrecht CA, Ruellas ACO, Paniagua B, Schilling JA, McNamara JA Jr, Cevidanes LHS. Three-dimensional characterization of root morphology for maxillary incisors. PLoS One 2017; 12:e0178728.
32. Jia P, Yang G, Hu W, Chung KH, Zhao Y, Liu M, et al. Comparison of in situ cone beam computed tomography scan data with ex vivo optical scan data in the measurement of root surface area. Oral Surg Oral Med Oral Pathol Oral Radiol 2019;128: 552-7.
33. Banodkar AB, Gaikwad RP, Gunjikar TU, Lobo TA. Evaluation of accuracy of cone beam computed tomography for measurement of periodontal defects: a clinical study. J Indian Soc Periodontol 2015;19:285-9.
34. Yang J, Li X, Duan D, Bai L, Zhao L, Xu Y. Cone-beam computed tomography performance in measuring periodontal bone loss. J Oral Sci 2019;61:61-6.
35. Walter C, Schmidt JC, Rinne CA, Mendes S, Dula K, Sculean A. Cone beam computed tomography (CBCT) for diagnosis and treatment planning in periodontology: systematic review update. Clin Oral Investig 2020;24:2943-58.
36. Patcas R, Müller L, Ullrich O, Peltomäki T. Accuracy of cone-beam computed tomography at different resolutions assessed on the bony covering of the mandibular anterior teeth. Am J Orthod Dentofacial Orthop 2012;141:41-50.
37. Icen M, Orhan K, Şeker Ç, Geduk G, Cakmak Özlü F, Cengiz Mİ. Comparison of CBCT with different voxel sizes and intraoral scanner for detection of periodontal defects: an in vitro study. Dentomaxillofac Radiol 2020;49:20190197.
38. Pauwels R, Faruangsaeng T, Charoenkarn T, Ngonphloy N, Panmekiate S. Effect of exposure parameters and voxel size on bone structure analysis in CBCT. Dentomaxillofac Radiol 2015; 44:20150078.
39. Pauwels R, Beinsberger J, Collaert B, Theodorakou C, Rogers J, Walker A, et al. Effective dose range for dental cone beam computed tomography scanners. Eur J Radiol 2012;81:267-71.